Fall 2013

Engineering a recombinant adenovirus system for the in vitro expression of ?-myosin

Kelly wun
University of Colorado Boulder

Engineering a recombinant adenovirus system for the *in vitro* expression of β-myosin

Kelly Wun

Defense Date: 31 October 2013

University of Colorado at Boulder

Department of Molecular, Cellular, and Developmental Biology

Thesis Advisor:

Dr. Leslie Leinwand, Department of Molecular, Cellular, and Developmental Biology

Thesis Defense Committee:

Dr. Jennifer Martin, Department of Molecular, Cellular, and Developmental Biology

Dr. James Goodrich, Department of Chemistry and Biochemistry

Abstract:

Over three hundred mutations in the molecular motor, myosin, cause a variety of cardiac and skeletal myopathies. One of our goals is to understand the functional implications of these mutations on the myosin molecule. Because myosin motors require a muscle cell context to be functional, the expression system for producing these proteins involves infecting differentiated muscle cells with recombinant adenoviruses. However, the growth of these adenoviruses in non-muscle cells is limited by an apparent toxic effect of myosin-production in HEK 293 cells during viral expansion. Thus adenovirus generation is the rate-limiting step in this process. To ameliorate this low adenovirus yield, we designed a system of repressing transgene expression in the virus packaging cell line by incorporating microRNA targets into the 3' UTR of the myosin transgene. As a proof of principle, using the kidney-specific miRNA, miR-192, multimers of the miR-192 target were introduced into a luciferase reporter through cloning. Subsequent experiments using the miR-192 reporter indicated an unexpectedly low expression of miR-192 in HEK 293 cells. Here, we use miR-192 and an artificial miRNA, miR-1-1sc to optimize the transgene repression in HEK 293 cultures through miRNA expressing cell lines. We expect transgene repression in this new miRNA-expressing, virus-packaging cell line will restore virus yields for generating sufficient β-myosin *in vitro*.

Table of Contents

Introduction:

I. Characterization of hypertrophic cardiomyopathy and mutations in β-myosin:

Heart disease is the number one killer of people in the United States and costs about $450 billion per year (cdc.gov). Hypertrophic cardiomyopathy (HCM), which is the leading cause of sudden death in young people, is the most common genetically inherited disease that affects one in every five-hundred people worldwide (Sivaramakrishnan, et al., 2009). The most common cause of inherited HCM is mutations in the cardiac motor protein, myosin (Svaramakrishnan, 2009). A condition called dilated cardiomyopathy (DCM) can also be caused by mutations in cardiac myosin, but these are far less common genetic cardiomyopathies.

An adult human heart is a fist-sized muscle with a hollow chamber that pumps five liters of blood every minute. With an average heart rate of seventy-two beats per minute, the heart will beat over one-hundred thousand times a day (Widmeier, et al., 378). The cells responsible for generating this pumping are the cardiac myocytes that are aligned and function in parallel arrays (Widmeier, et al., 366). Meanwhile, fibroblasts also make up a large portion of the cells in the heart and form the extracellular matrix that gives the heart its flexible yet durable structure. While stem cells and pacemaker cells represent a small percentage of the cells in the heart, these cells have crucial roles (Widmeier, et al., 368). Pacemaker cells participate in the cardiac conduction system by maintaining steady and synchronous beat; the stem cells function in a limited capacity to replace dead cells and repair injury (Widmeier, et al., 360-380).

Myocytes function as the primary contractile cell in the heart and the organized sarcomeres within these cells are the functional contractile units. Actin and myosin filaments arranged in parallel form these repeating sarcomeric units. In the presence of ATP and Ca^{2+}

in vivo, myosin will transiently bind actin and undergo a power stroke by hydrolyzing ATP to ADP and then release actin upon binding a new molecule of ATP. Myosin is essential for cardiac contractility; it is a heterohexamer composed of 2 heavy chains and 2 pairs of non-identical light chains. Of the ten myosin isoforms in humans, 90% of the myosin in the heart is the β isoform, which has been shown to have more than three hundred mutations that cause cardiomyopathy. Most of these mutations have been linked to HCM and less frequently to DCM and most, if not all, current therapeutics target pathways downstream of the sarcomere as opposed to directly targeting the mutant sarcomeric contractile proteins (Sivaramakrishnan, et al., 2009). Interestingly, depending on the disease, people with mutant myosins may exhibit increased (HCM) or decreased (DCM) contractility and ideally should be treated accordingly by potentially distinct therapeutics.

The most common mutations that we will be studying in β-myosin are the common HCM-causing mutations, R403Q and R453C, which are located in the MyHC motor or S1 domain. Because muscle myosin motors require muscle-specific chaperones to fold properly and therefore be active enzymes, these recombinant molecules must be expressed in differentiated muscle cells. The β-myosin motor domain from amino acids 1-808 was engineered in the lab into the adenoviral expression constructs. Tail domains were excluded because these domains form insoluble aggregates that make solution biochemical studies difficult. In order to study these mutants, these proteins must be expressed and purified in large quantities followed by measurement of enzyme kinetics via stopped flow techniques, the *in vitro* motility assay, and the ATPase assay. However, the current method of generating these β-myosin mutant proteins requires amplifying the virus in non-muscle, virus-permissive HEK 293 cells. For unexpected reasons, the expression of recombinant muscle myosin motors appears to be toxic to these cells,

limiting our ability to grow reasonable amounts of these viruses to infect muscle cells. Therefore, adenovirus growth is the rate-limiting step in this process.

II. Adenovirus infection of the cell:

Adenoviruses are approximately 90nm, nonenveloped, icosahedral viral particles that replicate within the nucleus of their host cell. The size of the double-stranded viral DNA is approximately 33-34 kilobases (kb) and pAdEasy-generated viruses can permit up to a 7.5 kb transgene. In humans, viral uptake into the cells requires the coxsackievirus and adenovirus receptor (CAR), which has been shown to be localized near tight junctions of the respiratory epithelium (Cohen, et al., 2001). CAR is characteristically expressed in respiratory epithelium, but the receptor is also present in other human tissues including heart, liver, pancreas, and intestines. Furthermore, adenovirus enters the cell by binding CAR and this virus particle docking permits integrin-activated, clathrin-coated endocytosis of the viral particle (Meier and Greber, 2004). Although virus entry to the cell has been studied to a degree where representative models have been constructed, viral particle escape from endosomes into the cellular cytoplasm and localization to the nucleus is not well understood. Studies have shown that adenovirus is transported by kinesin to the nucleus where the viral genome is activated and viral replication occurs (Cohen, et al., 2001). Prolonged virus replication through the lytic cycle results in host cell death and release of the viruses.

III. β-myosin expression in the pAdEasy recombinant adenoviral expression system:

The current method of generating recombinant adenovirus utilizes the pAdEasy system in which the adenovirus, serotype 5, viral genome was engineered to lack the E1 and E3 domains. Loss of E1 renders the viruses incompetent of replication *in vivo* and *in vitro* because the E1A genes are the immediate early genes required for initiation of viral replication. E3 is required for

in vivo growth but not *in vitro* because E3 expression produces proteins that aid in virus evasion from immune detection. Furthermore, the pAdEasy system requires competent virus packaging cells that complement for the loss of E1 in the viral genome. Hence, the HEK 293 cell line that was generated in the 1970's by transforming the cells with sheared DNA from adenovirus serotype 5 rendered these cells suitable for adenovirus replication by incorporating the viral E1 domain into the host cell chromosome 19. The HEK 293 cell line complements the virus replication cycle because the E1 products function in trans to initiate viral genome replication (Shaw, et al., 2002).

The current recombinant adenovirus protocol requires the incorporation of a gene of interest into the pShuttle-CMV vector and this resultant construct is linearized and transformed in recA-positive, pAdEasy-containing BJ5183 Escherichia coli cells. The recA-positive cells are necessary for homologous recombination of the linearized, pShuttle-CMV with pAdEasy and recombinants are selected using kanamycin. The subsequent recombinants are grown in overnight cultures and the recombinant pAd-plasmid is extracted and linearized for transfection into HEK 293 cells (Figure 1).

The pAdEasy adenoviral expression system is extremely useful for a wide spectrum of transgenic viral expression targets; however, the system is time-consuming and does not effectively generate adequate plaque-forming units when the β-myosin S1 domain or its engineered mutants are incorporated as the transgene compared to many other transgenes such as GFP or β-galactosidase. The low viral yields following transfection of linearized pAd-plasmid from the pAdEasy system presents a major challenge to our efforts to effectively and rapidly produce β-myosin protein for functional studies and stands as the rate limiting step for this *in vitro* β-myosin expression process. Hence, our goal in this project is to create and isolate HEK

293 cell lines that express microRNAs targeted to the myosin transgene bearing microRNA binding sites to downregulate transgene expression and increase viral particle generation in HEK 293 cells.

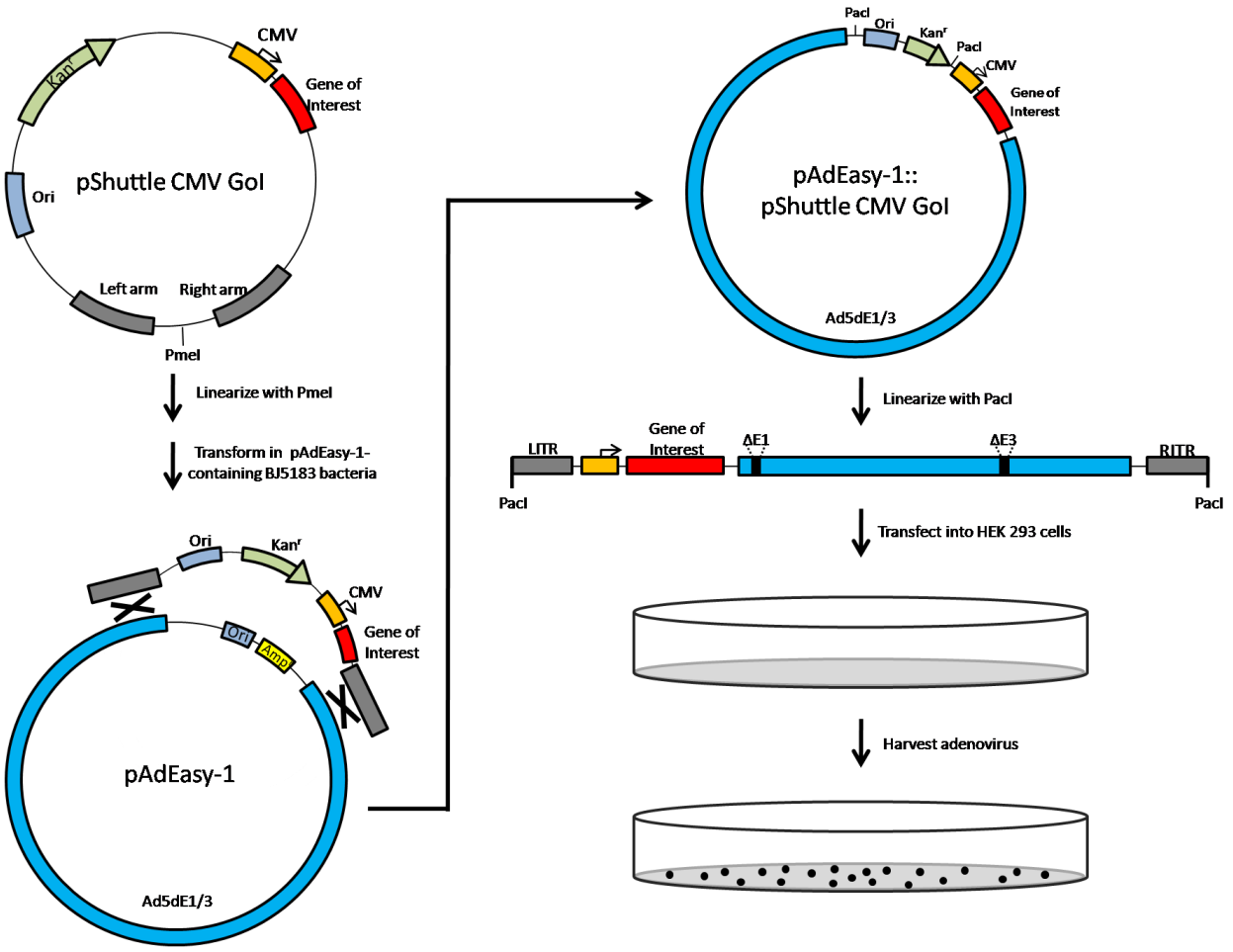

Figure 1: The pAdEasy adenoviral expression scheme. The gene of interest is cloned into the pShuttle-CMV GoI (Gene of Interest) construct downstream of the cytomegalovirus (CMV) promoter. The resulting plasmid is linearized with PmeI and transformed into pAdEasy-1-containing BJ5183 recA-positive cells, which will mediate homologous recombination of the linearized pShuttle construct with the corresponding region of pAdEasy-1 and confer kanamycin resistance to successful clones. The resulting construct, pAdEasy-1:: pShuttle-CMV GoI is linearized with PacI and transfected into the HEK 293 cell line where virus is expressed and later harvested. Adapted from He, et al., 1998.

IV. miR-192 and miR-1-1sc knockdown of transgene expression during virus generation:

The inability to generate high yields of virus is the bottleneck in expressing β-myosin motor domains. Accordingly, we are designing and implementing a β-myosin adenoviral expression system that utilizes microRNA targeting for downregulation of the myosin transgene expression in the virus-packaging, HEK 293 cell line in order to produce enough virus for subsequent infection of myogenic C_2C_{12} myoblasts. Based on findings of the kidney-specific miRNA, miR-192, miR-192 targets can be used to specifically knockdown transgene expression though transcript binding to the endogenous miRNA (Sun, et al., 2004). Complete complementary binding of miR-192 to its target through the RNA-induced silencing complex (RISC) mediates myosin transgene mRNA silencing by RISC binding to the 3'UTR at the complementary miRNA binding site and cleavage of the transcript resulting in exposed 5' and 3' ends on the mRNA transcript, followed by rapid RNA transcript degradation.

In the event that the miR-192 approach proves ineffective, miR-1-1sc is another potential miRNA that can be used to knockdown β-myosin transgene expression during virus generation because this miRNA and its target sequences are synthetic. The miR-1-1sc was designed by Dr. Kristen Barthel to lack homology to other known miRNAs and the expression vector, pcDNA3.1 miR-1-1sc, along with its target, psiCheck™2 miR-1-1sc, have been validated for activity. By integrating either miR-192 or miR-1-1sc targets into the 3'UTR of the myosin transgene in the viral genome and by generating cell lines to express either of the miRNAs, we expect that transgene expression will be repressed and permit virus assembly.

Methods & Procedures:

I. Multimerization of the miR-192 target and incorporation into psiCheck2:

A single miRNA target of miR-192 was developed based on the miR-192 sequence *in silico.* The miR-192 target was integrated into the pUC19 backbone using the HinDIII and EcoRI restriction sites (Figure 2a). Subsequent clones were picked and screened using PvuII on a 2% agarose gel for the presence of a molecular weight increase in the small fragment in comparison to the PvuII-digested parent plasmid.

The reiterations of the miR-192 targets were all constructed using a combination of XmnI/NheI digests and XmnI/XbaI digests of the miR-192-containing pUC19 plasmids (Figure 2b). The overhangs created by NheI and XbaI are convenient because they complement each other; by exploiting this feature, reiterations of the miR-192 target were created in series (Figure 2b). By gel purifying the digested XmnI-NheI and XmnI-XbaI pUC19 fragments that contained the miR-192 targets and ligating the fragments to each other, the number of miR-192 targets are effectively doubled after each round of multimerization until there were thirty-two copies of the target in pUC19.

Using the psiCheck™2CCND1 vector that was generously provided by Dr. Kristen Barthel, the miR-192 targets from pUC19 miR-192 x8, pUC19 miR-192 x16, and pUC19 miR-192 x32 were all moved into the psiCheck™2 vector. Using NotI and XhoI restriction sites, the miR-192 targets were incorporated into the 3' UTR of the renilla luciferase gene of psiCheck™2 (Figure 3).

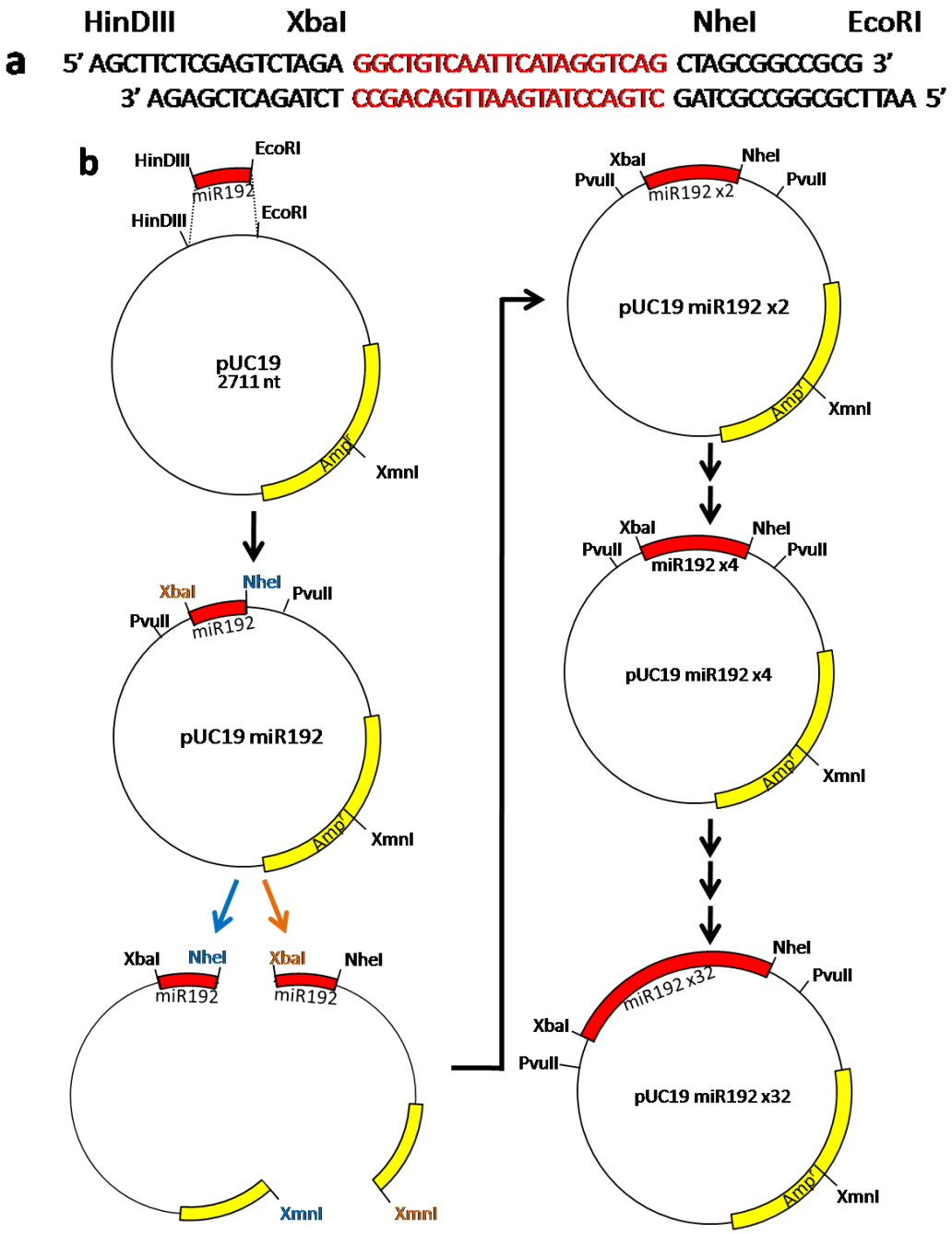

Figure 2: The miR-192 target development. a) The annealed oligonucleotides that comprise the miR-192 target. The top strand of the indicated region (red text) shows the miR-192 target sequence. The overhang on the left is the sticky end of HinDIII and the overhang on the right is the EcoRI sticky end. b) The plasmid diagram illustrates the incorporation scheme of the miR-192 target into the pUC19 vector by using HinDIII and EcoRI digestion of the vector and subsequent incorporation of the miR-192 oligonucleotides by ligation. Ligating the miR-192-containing pUC19 fragments (as shown in the bottom left schematic) doubles the number of miR-192 targets through each cycle. The multimerizing process continued until thirty-two copies of the miR-192 target were incorporated into pUC19.

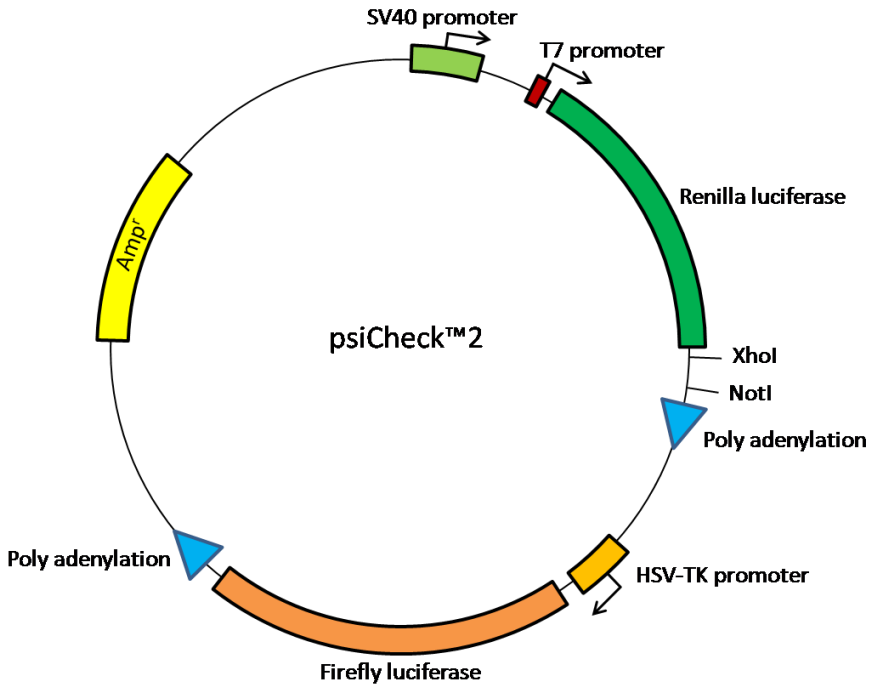

Figure 3: The plasmid construct of psiCheck™2. The significant components are noted. The miR-192 targets were incorporated into the 3' UTR of the renilla luciferase gene using XhoI and NotI restriction sites.

II. Transfection of HEK 293 cells:

For each transfection in HEK 293 cells, a total of 5µg of DNA in 150µL of sterile water was mixed with 50µL of 1M $CaCl_2$. While maintaining a constant bubbling in 200µL of 2x Hepes-buffered saline (HBS) using a plugged Pasteur pipette attached to a pipette aide, the 200µL DNA/$CaCl_2$ solution was added dropwise to thoroughly mix the precipitate solution in a 1.5mL microfuge tube. Finally, the 400µL of the DNA precipitate solution containing DNA, $CaCl_2$, and HBS was added dropwise to the 60mm HEK 293 cell plates and the plates were stored at 37°C and 5% CO_2. The media was changed five hours after the transfection by washing the plates with 1x phosphate-buffered saline (PBS) + EDTA and replaced with fresh growth media (Dulbecco's Modified Eagle Medium (DMEM) + 10% fetal bovine serum (FBS) + penicillin-streptomycin + L-glutamine and stored at 37°C and 5% CO_2). The cells were washed

with PBS without EDTA and harvested using passive lysis buffer from the Dual-Luciferase Reporter Assay® system two days post-transfection. The HEK 293 cells were seeded at a 1:3 split ratio such that cultures were transfected the following day and were confluent by the time the cells were harvested.

All HEK 293 cells were cultured in growth media and stored in 37°C and 5% CO_2.

III. Transfection and differentiation of C_2C_{12} myoblasts into myotubes:

For C_2C_{12} transfections, the DNA precipitate is prepared and added to the 60 mm dishes the same way as for the HEK 293 transfections. C_2C_{12} cells were maintained in growth media at 37°C and 5% CO_2 in order for the myoblasts to grow to confluency. After cultures were confluent at approximately two days post-transfection, the culturing media was changed to differentiation media (DMEM + 2% horse serum (HS) + penicillin-streptomycin + L-glutamine) to induce C_2C_{12} myoblast differentiation into myotubes. Three days after the differentiation media was added, the cultures were harvested using the passive lysis buffer from the Dual-Luciferase Reporter Assay® system.

The C_2C_{12} myoblasts were cultured in growth media and stored at 37°C and 5% CO_2.

IV. Luciferase assay of psiCheck2 transfections:

Dual-luciferase assays tested for the knockdown of renilla luciferase expression relative to firefly luciferase expression. These assays were performed on miR-192- and miR-1-1sc-containing psiCheck™2 transfected cell culture dishes. As mentioned previously, the media from transfected, 60mm cell cultures was aspirated, the cells washed with 1x PBS without EDTA, and the cultures were harvested using 400µL of 1x passive lysis buffer as prescribed in Promega's Dual-Luciferase Reporter Assay® system. The lysis buffer-containing plates were gently rocked

at room temperature for 15 minutes and then the lysates were transferred into 1.5mL microfuge tubes.

The renilla:firefly ratios were obtained using the dual-luciferase mode on the Turner Designs TD-20/20 luminometer. 50µL of Luciferase Assay Reagent II (LAR II) was aliquoted into the assay vials, then 10µL of cell lysate was added, briefly vortexed, and the luminescence was immediately measured in the luminometer for ten seconds that was preceded by a three-second measurement delay. After the measurement was complete, 50µL of Stop & Glo® reagent was added the tube then the tube was briefly vortexed, and the second luminescence measurement was recorded again for ten seconds with a three-second measurement delay (Figure 4). Trials of each lysate were performed in technical triplicates. The final ratio of renilla/firefly luciferase indicates the degree of expression knockdown relative to a control psiCheck™2 construct.

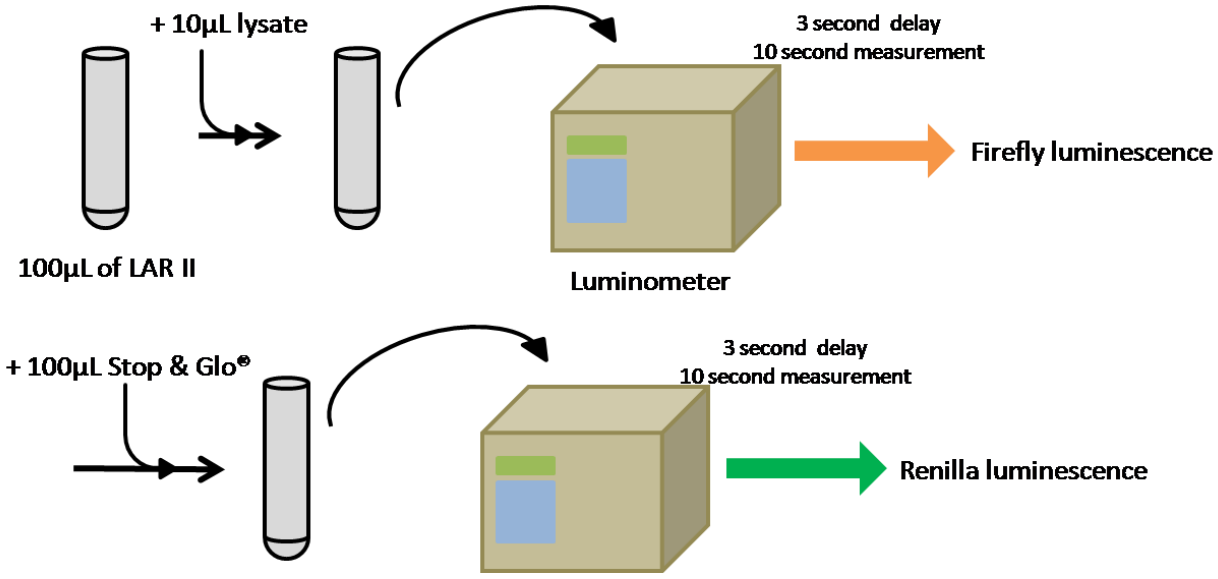

Figure 4: Schematic of the luciferase assay. Firefly luminescence was measured for ten seconds with a three second delay immediately after 10µL of cell lysate was added to the 50µL of LAR II and briefly vortexed. After the first measurement was complete, 50µL of Stop & Glo® was added to the vessel to stop the firefly luminescence and initiate the renilla luminescence. The sample was briefly vortexed and the second luminescence measurement was promptly recorded.

V. Development of a microRNA-expressing HEK 293 cell line:

A completely artificial microRNA expression vector, pcDNA3.1 miR-1-1sc, and the corresponding target construct, psiCheck™2 miR-1-1sc x2, were graciously provided to us by Dr. Kristen Barthel. pcDNA3.1 miR-1-1sc was transfected into HEK 293 cell cultures that were seeded 1:20, clones were selected for having G418 resistance, and cell lines were picked and grown. Isolated cell lines were transfected with psiCheck™2 miR-1-1sc x2 and the expression downregulation of the most robust miR-1-1sc-expressing cell line was cultured and expanded.

In effort to express miR-192, we designed an expression vector using pcDNA3.1 and introduced the miR-192 sequence. First, the annealed oligonucleotides for the 5' portion of the miR-192 gene were incorporated into pcDNA3.1 using a NheI and EcoRI digest followed by subsequent ligation of the annealed oligonucleotides into the vector. For the 3' segment of the miR-192 gene, oligonucleotides were extended using the other oligonucleotide as a template in one cycle of PCR. The subsequent elongation products were digested with MfeI and BamHI and inserted into the EcoRI- and BamHI-digested pcDNA3.1 miR-192a vector by exploiting the complementary sticky ends of MfeI and EcoRI. Candidate clones were screened by the loss of the BstXI restriction site and by the appearance of a 408bp band as opposed to a 353bp band.

Co-transfections of psiCheck™2 miR-192 x2, psiCheck™2 miR-192x8, psiCheck™2 miR-192x16, and psiCheck™2 miR-192x32 with pcDNA3.1 miR-192 or with pcDNA3.1 miR-1-1sc using a total of 5µg of DNA (1µg pcDNA3.1 expression vector + 4µg psiCheck™2 reporter) were performed in HEK 293 cells that were plated 1:3 on 60mm culture plates. The cultures were washed and lysed with passive lysis buffer, and the expressions of firefly and renilla luciferase were measured using the Dual-Luciferase Reporter Assay® system.

Results:

I. Verification of miR-192 multimer formation:

Following each reiteration of the miR-192 target into the pUC19 backbone, clones were screened using PvuII. Positive clones were identified by having an increased molecular weight in the smaller fragment compared to the parent construct on a 2% agarose gel (Figure 5). The plasmid DNA from these positive clones were digested, purified, and ligated together using the same XmnI-NheI and XmnI-XbaI scheme to double the number of targets.

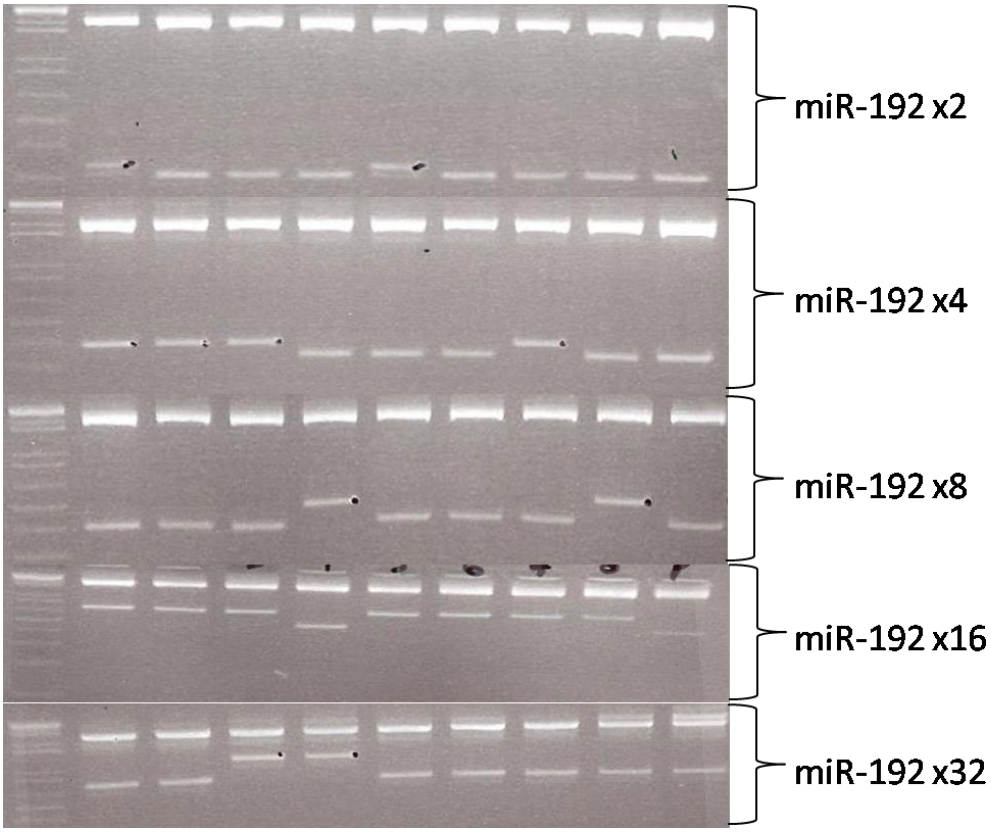

Figure 5: Images of the PvuII-digested candidate clones run on 2% agarose gels. The label to the right of each gel indicates the multimeric construct screened. Positive clones were selected based on have a larger "small" band compared to the digested parent construct (rightmost lane in each gel). The larger band represents the pUC19 backbone at approximately 2.4kb.

II. Expression knockdown mediated by miR-192 targets by endogenous miR-192:

An initial experiment was performed using two copies of the miR-192 target directly in the psiCheck™2 vector (data not shown). From the initial expression knockdown, psiCheck™2 miR-192 x8, psiCheck™2 miR-192 x16, and psiCheck™2 miR-192 x32 were transfected into HEK 293 cultures and the subsequent luciferase assay showed increasing reductions in the renilla/firefly ratios as more miR-192 targets were present (Figure 6a). In effort to validate the system, we repeated the previous experiment in C_2C_{12} cells using the appropriate culturing and differentiating conditions. These data show significant reductions in the renilla/firefly ratios that are further reduced as the number of miR-192 target copies increases (Figure 6b).

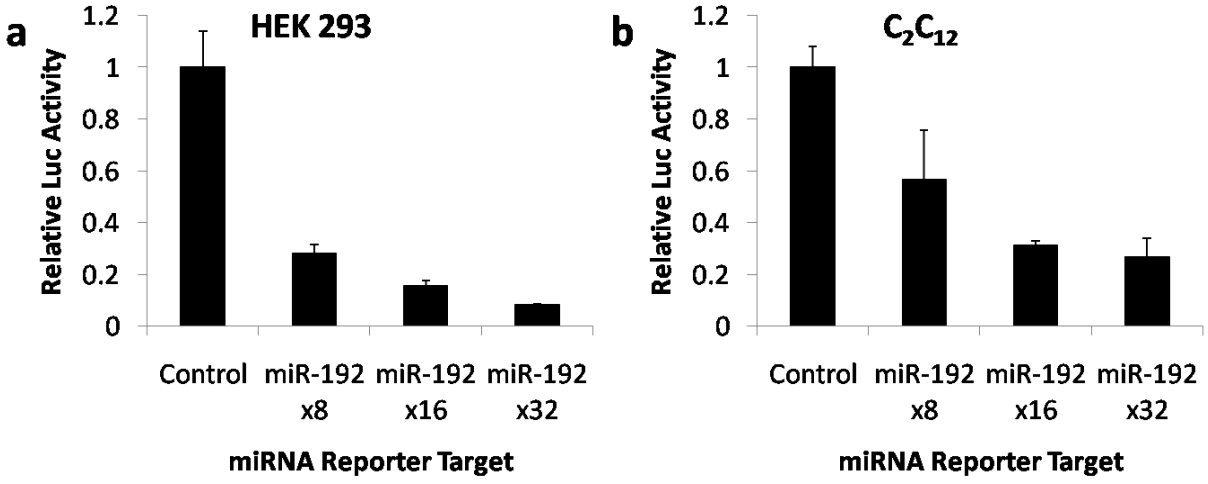

Figure 6: Renilla/firefly luciferase ratios were normalized against the control reporter construct. a) The graph shows the expression knockdown in HEK 293 cultures when transfected with the multimerized miR-192 targets. b) The same transfection setup from a) was performed in C_2C_{12} myoblasts. Both a) and b) show increased miRNA-induced silencing to the increasing number of miR-192 targets.

From the previous experiments, we conclude that miR-192 is not highly expressed in HEK 293 cells. Therefore, the expression vectors pcDNA3.1 miR-1-1sc or pcDNA miR-192 were co-transfected into HEK 293 cells with psiCheck™2 miR-192 x2, psiCheck™2 miR-192 x8, psiCheck™2 miR-192 x16, and psiCheck™2 miR-192 x32. When miR-192 was co-

transfected with the respective miR-192 targets and cells were assayed using the dual luciferase assay, all but the miR-192 x2 showed significant downregulation compared to the expression ratio from the miR-1-1sc x2 target (Figure 7). But when miR-1-1sc was expressed with the same reporters, the degree of knockdown was the same as in the miR-192 expression in the miR-192 x8, miR-192 x16, and miR-192 x32 targets but there was significant knockdown in miR-1-1sc (Figure 7b). The miR-1-1sc expression knockdown in its respective target is consistent with the previous validation characterized by Dr. Kristen Barthel.

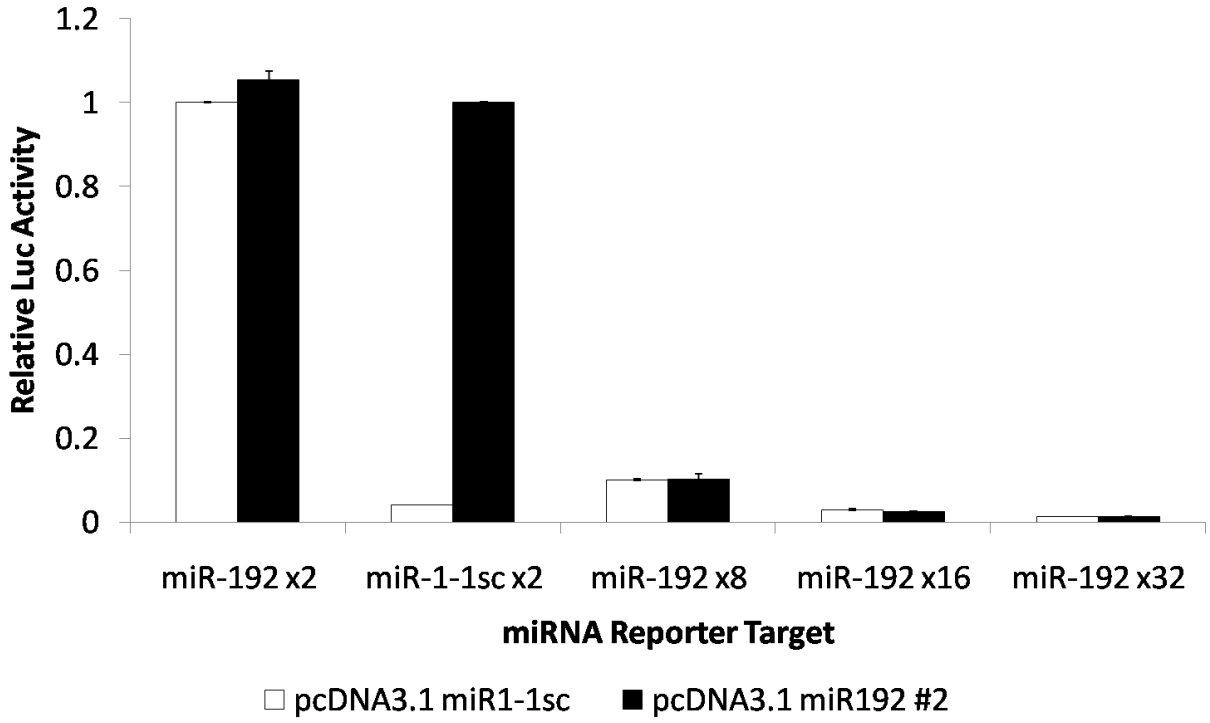

Figure 7: The expression knockdown during miR-192 or miR-1-1sc expression in HEK 293 cells. During miR-192 expression (black bars) of a particular clone of the pcDNA3.1 miR-192 construct, there is no significant miRNA-induced silencing from miR-192 x2 compared to miR-1-1sc x2 but there is a significant difference in miR-192 x8, miR-192 x16, and miR-192 x32. miR-1-1sc expression (white bars) leads to a significant silencing effect measured by the miR-1-1sc x2 reporter and the same degree of silencing is present in miR-192 x8, miR-192 x16, and miR-192 x32 reporters. In a direct comparison of the miR-192 x8, miR-192 x16, and miR-192 x32 ratios, there is no difference between the each respective miRNA-induced knockdown whether miR-1-1sc or miR-192 was expressed.

Discussion:

I. Validation of the endogenous miR-192-induced silencing:

Based on the results of the endogenous miR-192-induced silencing experiment, HEK 293 cells do not appear to express miR-192 at an appreciable level despite miR-192 being a kidney-specific miRNA and HEK cells being derived from human embryonic kidney. Additionally, the silencing induced by miR-192 is amplified through increasing the number of miR-192 binding sites. When comparing this dose-dependency between HEK 293 and C_2C_{12} cells, the same patterns are observed and this indicates that the miR-192 targets are being bound by miR-192 or perhaps another non-specific miRNA. There is a possibility in the case of non-specific miRNAs that another endogenous miRNA is binding across the junctions between one miR-192 target to the next. On the other hand, the miR-192 targets in the mRNA transcripts may be destabilizing these target-bearing transcripts leading to degradation without miRNA-mediated silencing.

For the adenovirus generation, the expression silencing in C_2C_{12} cells in response to the miR-192 targets is undesirable (Figure 6b). Incorporation of these miR-192 iterations would result in reduced transgene expression in HEK 293 cells, which may rescue virus growth, but the expression knockdown seen in C_2C_{12} myotubes by miR-192-mediated silencing of the transgene will reduce β-myosin production, making the endogenous miR-192-induced silencing ineffective. These data suggest that the endogenous levels of miR-192 expression is low in both cell lines because two copies of miR-1-1sc targets were able to induce approximately 20-fold reductions in the miR-1-1sc activity when miR-1-1sc was expressed (Figure 7). miR-192 was initially described to be a kidney-specific miRNA and despite the origin of HEK 293 cultures, these cells do not appear to express miR-192 beyond a background level because the degree of expression silencing in both HEK 293 cells and C_2C_{12} myoblasts was not significantly different. Despite the

lack of miR-192 expression in HEK 293 cells, these reiterated miRNA targets in psiCheck™2 may be a highly sensitive reporter system that can detect background levels of miRNA in transfected cells.

II. miRNA expression in transfected HEK 293cultures:

The miR-192 expression in HEK 293 cells by transfecting cells with pcDNA3.1 miR-192 in parallel with miR-1-1sc expression showed no difference in expression knockdown by miR-192-induced silencing whereas miR-1-1sc-induced silencing was as expected (Figure 7). Since the miR-192 targets contain many more iterations than in miR-1-1sc x2 and yet the ratios of the miR-192 x8, miR-192 x16, and miR-192 x32 are not different when expressing either miR-192 or miR-1-1sc, this suggests that the pcDNA 3.1 miR-192 expression vector is not producing functional miR-192 that can target the reiterated miR-192 targets. Although the miR-192 gene was partially constructed using PCR, the newly introduced gene was not sequenced. Consequently, the expression vector may not be the correct construct.

Future Directions:

I. Verification of psiCheck™2 CCND1 as a control target:

Based the results obtained while co-transfecting pcDNA3.1 miR-192 with the control construct psiCheck™2 CCND1 (Cyclin D1), its expression levels were significantly reduced compared to the miR-1-1sc x2 reporter. This lead us to realize that the CCND1 3' UTR is not an adequate control because its expression was being knocked down when no repression was ideal. So to validate that psiCheck™2 CCND1 is not an adequate control, another set of co-transfections must be done to show that the CCND1 3'UTR is targeted for repression. Instead of using miR-1-1sc x2 renilla/firefly ratio as the control during miR-192 expression, the construct without any cloning modifications in the renilla luciferase 3' UTR, psiCheck™2 empty will be used instead. By co-transfecting psiCheck™2 empty with the previously used pcDNA3.1 miR-192 expression construct, psiCheck™2 miR-1-1sc x2 can be validated as a control in the miR-192 expression experiment.

II. Measurement and validation of miR-192 in transfected and non-transfected HEK 293 cultures:

Quantification of the miR-192 levels in both transfected and non-transfected by qPCR will indicate the miR-192 activity in each experimental group. By measuring and comparing the miR-192 levels in pcDNA3.1 miR-192-transfected and non-transfected HEK 293 cultures, the candidate pcDNA3.1 miR-192 clones can be selected and validated for producing mature and functional miR-192.

RNA from the following pcDNA3.1-transfected HEK 293 cultures will be isolated: no pcDNA3.1, pcDNA3.1 empty, and two pcDNA3.1 miR-192 from clone #2 and #5. As a positive control, RNA isolated from homogenized mouse kidney will verify miR-192 activity in this assay. From miRbase, the mature mouse miR-192 miRNA is the same as mature human miR-192.

III. Validation of a stable viral expression system using miRNAs:

Transient transfections of the expression vectors with their respective reporter constructs provide a measurement of transgene knockdown, but the luciferase assay cannot predict other outcomes that may affect virus growth. To ensure that transgene silencing by miRNA targeting is effective and stable in the context of virus production, we must grow these recombinant adenoviruses in this miR-1-1sc expressing cell line. By validating whether recombinant β-myosin adenoviruses can grow stably at high yields in the miR-1-1sc expressing cell line, we will show if transgene repression is effective and whether apparent buildup of misfolded β-myosin was the toxic agent to the cell.

IV. Virus growth system for β-myosin S1 domain production and protein purification:

Recombinant adenoviruses will be produced after the miRNA transgene knockdown system is complete and validated. Viruses grown from DNA transfections into HEK 293 cells will infect additional HEK 293 cultures to amplify our quantity of adenovirus. When large quantities of viruses are acquired, C_2C_{12} myoblasts will be infected for β-myosin generation. However, C_2C_{12} adenoviral infectivity is low as a result of low CAR expression. As a potential solution, CAR expression, whether constitutively or conditionally, may remedy the low infectivity because adenovirus infectivity is limited by CAR localization to the cell surface (Cohen, et al. 2001).

Improved β-myosin viral yields in conjunction with increased C_2C_{12} infectivity, is expected to require less time to generate adequate quantities of β-myosin for subsequent assays. These β-myosin S1 domains will be purified using affinity chromatography for the C-Tag on the C-terminal end.

V. Assaying β-myosin kinetics in the presence of a potential therapeutic drug:

Purified recombinant β-myosin will be subjected to various assays to quantify the enzyme kinetics of the mutants and wild-type proteins. However, myosin activity requires actin for assays including the *in vitro* motility. G-actin is purified from several pounds of raw chicken breast by grinding, dehydrating, and finally purifying the actin over the course of two days. Actin can be labeled with a fluorescent tag, induced to polymerize, and subjected to the *in vitro* motility assay. β-myosin is fixed to a slide and the labeled F-actin is visualized using microscopy as the filaments traverse across the image field in the presence of ATP. The distance that a labeled actin filament travels over a period of time is representative of the myosin kinetics. These kinetics measurements will be taken in the presence of a drug, omecamtiv mecarbil, and other potential therapeutic drugs. Other experiments including stopped flow and ATPase assays will provide more insight into the mutant and wild-type β-myosin enzyme kinetics.

Acknowledgements:

Many thanks to Dr. Leslie Leinwand for allowing me to continue researching heart-related pathologies and diseases and pursue this honors thesis. It has been a pleasure to work with the Leinwand lab since October 2012. I am truly grateful to Dr. Timothy McKinsey and his lab for connecting me with Leslie. I would like to thank Dr. Steve Langer and Carlos Vera for guiding me through this project and overseeing my progress. I am grateful to Uriel Bulow and Josephine Imparato for aiding and contributing significantly to the cloning and cell culture. I would like also like to thank Dr. Kristen Barthel for providing the miRNA idea for this project in addition to providing us several constructs to generate a new cell line and the corresponding reporter constructs. Thanks to Ariana Combs for maintaining the tissue culture and her contribution towards developing the new cell line. I want to thank Dr. Jennifer Martin and Dr. James Goodrich for being on my defense committee.

Special thanks to my family and friends that has supported me for all these years. I am most appreciative to have Clarinda Hougen's support during these past few years.

References

Cohen, C. J., Shieh, J. T. C., Pickles, R. J., Okegawa, T., Hsieh, J., Bergelson, J. M., (2001). The coxsackievirus and adenovirus receptor is a transmembrane component of the tight junction. *PNAS*, 98(26) 15191-15196.

He, T., Zhou, S., Da Costa, L. T., Yu, J., Kinzler, K. W., Volgelstein, B., (1998). A simplified system for generating recombinant adenoviruses. *PNAS*, 95, 2509- 2514.

Heidenreich, P. A., Trogdon, J. G., Kavjou, O. A., Butler, J., Dracup, K., Ezekowitz, M. D., Finkelstein, E. A., Hong, Y., Johnston, S. C., Khera, A., Lloyd-Jones, D. M., Nelson, S. A., Nichol, G., Orenstein, D., Wilson, P. W.F., Woo, Y. J., (2011). Forecasting the Future of Cardiovascular Disease in the United States: A Policy Statement From the American Heart Association. *Circulation*, 123, 933-944.

Meier, O., Greber, U. F., (2004). Adenovirus endocytosis. *The Journal of Gene Medicine*, 6, S152-S163.

Sivaramakrishnan, S., Ashley, E., Leinwand, L., Spudich, J. A., (2009). Insights into Human β-Cardiac Myosin Function from Single Molecule and Single Cell Studies. *Journal of Cardiovascular Translational Research*, 2(4), 426-40.

Shaw, G., Morse, S., Ararat, M., Graham, F. L., (2002). Preferential transformation of human neuronal cells by human adenovirus and the origin of HEK 293 cells. *The FASEB Journal*, 16(8), 869-71.

Sun, Y., Koo, S., White, N., Peralta, E., Esau, C., Dean, N. M., Perera, R. J., (2004). Development of a micro-array to detect human and mouse microRNAs and characterization of expression in human organs. *Nucleic Acids Research*, 32(22), 1-6.

Widmaier, E. P., Raff, H., Strang, K. T., *Vander's Human Physiology: The Mechanisms of the Body Function* (McGraw-Hill. ed. 11, 2007), pp 360-380. [Eleventh edition]

[28 August 2013] Heart Disease Facts.Heart Disease.[Online]. Available: http://www.cdc.gov/heartdisease/statistics.htm. [24 October 2013].

(31 August 2010) Adenoviruses. MicrobiologyBytes. [Online]. Available: http://www.microbiologybytes.com/virology/Adenoviruses.html. [21 October 2013].

Supplemental Data

I. Oligonucleotides:

miR-192 x2 target:

miR-192 (5' to 3') (miR-192 targets indicated):TCGAGGGCTGTCAATTCATAGGTCAGAAGGCTGTCAATTCATAGGTCAGTCTAGA

miR-192 (5' to 3'):
GGCCTCTAGACTGACCTATGAATTGACAGCCTTCTGACCTATGAATTGACAGCCC

miR-192 multimerizing target:

miR-192 H3-RI_T (5' to 3') (miR-192 target indicated):

AGCTTCTCGAGTCTAGAGGCTGTCAATTCATAGGTCAGCTAGCGGCCGCG

miR-192 H3-RI_B (5' to 3'):

AATTCGCGGCCGCTAGCTGACCTATGAATTGACAGCCTCTAGACTCGAGA

miR-192 expression gene:

miR-192 SP Nhe-EcoRI (5' to 3'): CTAGCCGAGACCGAGTGCACAGGGCTCTGACCTATG

miR-192 ASP Nhe-EcoRI (5' to 3'): AATTCATAGGTCAGAGCCCTGTGCACTCGGTCTCGG

miR-192 SP Mfe-BamHI (5' to 3'):
GCGCAATTGACAGCCAGTGCTCTCGTCTCCCCTCTGGCTGCCAATTCCATAGGTC

miR-192 ASP Mfe-BamHI (5' to 3'):
TATAGGATCCGCTGGCATTGAGGCGAACATACCTGTGACCTATGGAATTGGCAG

miR-192 Mfe-BamHI PCR elongation:

Cycling:

30 seconds @ 98°C
10 seconds @ 98°C
30 seconds @ 62.5°C
75 seconds @ 72°C
} 1 cycle
30 seconds @ 72°C